ADVANCED INTELLIGENT SYSTEMS
Open Access
www.advintellsyst.com

Human–Machine Collaboration for Automated Driving Using an Intelligent Two-Phase Haptic Interface

Chen Lv, Yutong Li, Yang Xing, Chao Huang, Dongpu Cao, Yifan Zhao, and Yahui Liu*

Prior to realizing fully autonomous driving, human intervention is periodically required to guarantee vehicle safety. This poses a new challenge in human–machine interaction, particularly during the control authority transition from automated functionality to a human driver. Herein, this challenge is addressed by proposing an intelligent haptic interface based on a newly developed two-phase human–machine interaction model. The intelligent haptic torque is applied to the steering wheel and switches its functionality between predictive guidance and haptic assistance according to the varying state and control ability of human drivers. This helps drivers gradually resume manual control during takeover. The developed approach is validated by conducting vehicle experiments with 26 participants. The results suggest that the proposed method effectively enhances the driving state recovery and control performance of human drivers during takeover compared with an existing approach. Thus, this new method further improves the safety and smoothness of human–machine interaction in automated vehicles.

1. Introduction

The development of automated roadway vehicles has generated increasing attention from both academia and industry in recent years. However, the development of highly automated vehicles or semiautonomous vehicles, where the driving task is exchanged periodically between human drivers and automated vehicle technologies, can be expected to precede the transition to fully autonomous vehicles.[1–3] The transition between human driving and automated driving modes represents a particular risk because human drivers may be preoccupied with a nondriving activity (NDA), and some time may be required for humans to recover a suitable level of driving performance required for safe control.[4–6] As such, guaranteeing safe, smooth, and swift control authority transitions between a human driver and the automated functionality of the vehicle is a critical issue in this technology.[7–9] This challenge requires new cross-disciplinary theory, analysis, and design approaches related to human–machine collaboration.

To address this problem, many studies with a focus on human factors have been conducted to investigate the key factors that influence takeover performance. It was found that the main key factors are the required takeover time, modality of the takeover request (TOR) signal, secondary task engagement, driver states, and driving conditions.[10–12] The effect of takeover time on driver reactions and control performance has been investigated.[13] The results showed that with a shorter TOR time, the participants reacted faster, but the takeover control performance worsened. The increase in takeover time was found to be heavily related to the level of cognitive workload occupied by secondary tasks.[14,15] Different modalities of the TOR signal were investigated in one study,[16] and the results showed that users' preferences for TOR modalities in highly automated vehicles depended on the urgency of the driving situation. The impact of traffic density on the takeover process was explored, and the results indicated that a high density of traffic flow would have a negative impact on both takeover time and post-takeover performance.[17] In addition, the driver's readiness and takeover ability were explored by modeling and estimation.[10,18–20]

In addition to the above human factor studies, advanced control methods have also been adopted to solve human–machine interaction issues for automated vehicles. In some studies, the

Prof. C. Lv, Dr. Y. Li, Dr. Y. Xing, Dr. C. Huang
School of Mechanical and Aerospace Engineering
Nanyang Technological University
50 Nanyang Ave, 639798 Singapore, Singapore
E-mail: lyuchen@ntu.edu.sg

The ORCID identification number(s) for the author(s) of this article can be found under https://doi.org/10.1002/aisy.202000229.

DOI: 10.1002/aisy.202000229

Prof. D. Cao
Mechanical and Mechatronics Engineering
University of Waterloo
Waterloo, ON N2L 3G1, Canada

Prof. Y. Zhao
School of Aerospace, Transport and Manufacturing
Cranfield University
Bedford MK43 0AL, UK

Prof. Y. Liu
School of Vehicle and Mobility
Tsinghua University
Beijing 100084, China

takeover strategy of instant control transfer from automation to driver was adopted even if the human was not ready for the required driving task.[13,21] A period of shared control was suggested as a promising solution to further enhance vehicle safety and comfort during handover.[22] Based on a novel definition of the cooperative state between automation and driver, a smooth control authority transfer from automated driving to manual driving with haptic shared control was developed.[23] The proposed strategy of authority transfer was realized by tuning the design gain, which was correlated with the driver's steering torque. The effects of different types of haptic steering torque on driving performance have also been studied.[12,24] The results indicated that a continuous haptic steering torque can improve the path-following performance of drivers during standard steering maneuvers. From the literature, there are many possible ways to handle driver–automation collaboration (such as handover) for automated vehicles utilizing haptic shared control. However, some of these methods are not associated with the model of a human driver. Taking the prediction of a driver's action into consideration may further benefit the performance of human–machine cooperation. The intention of the driver was considered within modeling and included in the objective function to minimize controller intervention during driver–automation shared control.[25] Similarly, some frameworks have been proposed and implemented in the design of haptic shared control and advanced driver assistance systems by integrating a dynamic model of the driver,[26–28] but the authorities allocated to humans and automation were fixed. Based on the above concepts, a new framework was developed based on a game theoretical model of human–machine interaction for dynamic role distribution.[19,29] Under this framework, different concepts of control transitions were developed for the takeover of automated vehicles and compared via human-in-the-loop experiments.[30] The test results indicated that the shared control-based methods were preferable to those with the immediate shutdown of automation. However, because human behavior was described by an optimal controller, imperfect driver behavior during the takeover process could hardly be captured. In addition, the dynamic adaptation of handover parameters as well as real-vehicle implementation and validation have not yet been fully addressed.

Although many technological achievements have been made in this field in the past, challenges in the human–machine interaction of automated vehicles, particularly for the automation-to-driver takeover process, still remain. These require the design of novel human–machine collaboration systems. During takeover, humans may need some time to recover from preoccupied secondary tasks to a suitable level of required driving performance. Naturally, their mental and physical states and readiness may vary, which have to be considered. Clearly, some types of guidance and assistance to human drivers are needed to ensure the safe, smooth, and swift completion of the handover. Thus, to further advance the approach for takeover control of automated vehicles, the present work develops a human–machine collaboration approach that provides necessary guidance and assistance to humans using an intelligent two-phase haptic interface, which is expected to adapt to the varying state and control ability of drivers during takeover.

As shown in **Figure 1**, during takeover transition, the proposed human–machine collaboration system modulates the

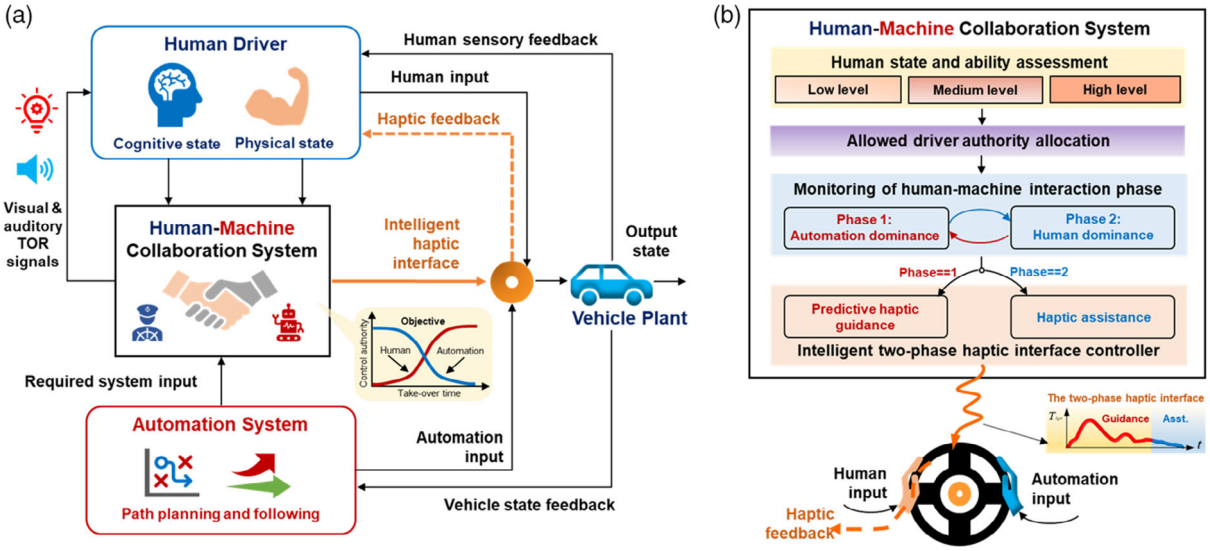

Figure 1. Architecture of the human–machine collaboration system with the intelligent haptic interface for automated driving. a) After perceiving the multimodal TOR signal, the human driver is required to take over control of the vehicle driven in the autonomous mode. During takeover transition, the proposed human–machine collaboration system modulates the automation's control efforts according to the driver's state and control action, providing an intelligent haptic steering interface to help the human driver take over control in a safe and smooth manner. With the gradual increase of the driver's input, automation's input decreases accordingly, and the handover process is expected to be completed gradually. b) The proposed system assesses the states and control ability of the driver in real time, deciding the maximum control authority (the upper bound) that could be allocated to the driver. In the meantime, based on the monitored status of the human–machine interaction process, the two-phase intelligent haptic torque is applied on the steering wheel. If the automation system dominates the control (in phase 1), then a haptic guidance torque will be provided based on the prediction of the driver's future behavior, helping the human driver apply an appropriate degree of steering torque. If the driver starts to dominate the control (in phase 2), then the functionality of the haptic interface will be switched from predictive guidance to assistance.

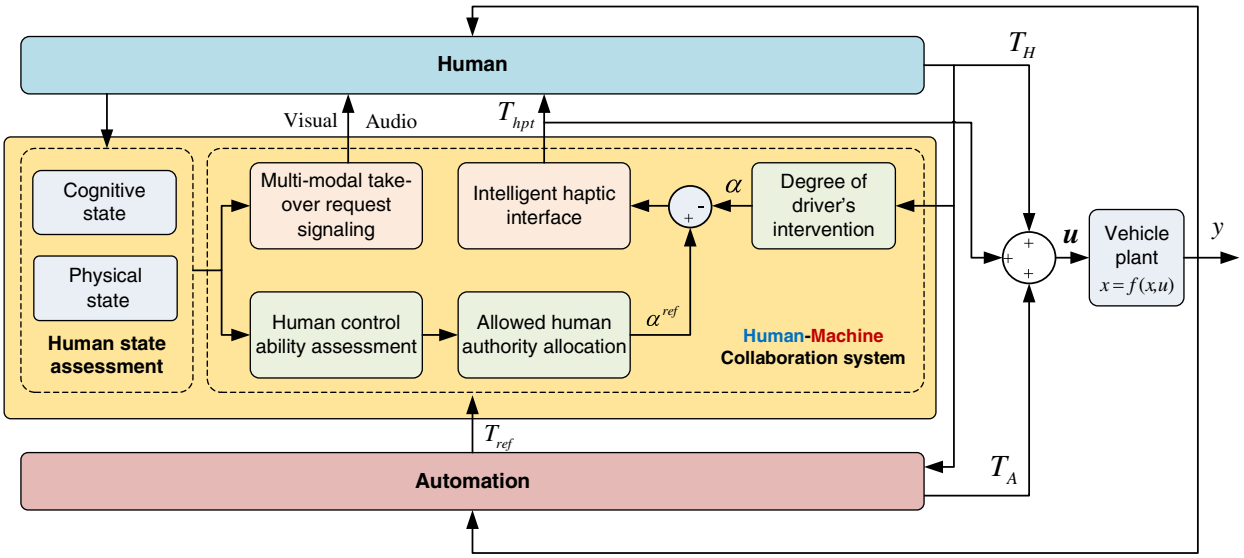

Figure 2. Control block diagram of the proposed human–automation collaboration system with the intelligent haptic interface. During the takeover process, an optimal sequence of control input T_{ref} will first be derived from the planned trajectory of the automated vehicle. In the meantime, the developed human–automation collaboration system assesses the driver's state and control ability in real time. Then, it decides how much control authority should be allocated to the human driver, gradually increasing this with the recovery of the driver's state and control performance. To do this, a human authority allocation module was designed to calculate the allowed driver authority α^{ref} in real time, based upon the driver's cognitive attention, neuromuscular state, and the required driving task. The real value of the driver's degree of intervention α will then be compared with the allowed one α^{ref}. The intelligent haptic feedback torque will then be generated on the steering wheel to minimize the deviation between α and α^{ref}. The haptic steering torque applied is expected to guide or assist the driver to use an appropriate degree of steering torque so as to gradually complete the overall handover process. Thus, during the automation–human takeover transition, the human and the machine dynamically share the control authority, jointly completing the required driving task. The steering torque contributed by the human driver takes up α% of the overall torque applied to the vehicle. Moreover, the input contributed by automation system, T_A, always compensates for the summation of the driver's actual torque and the haptic torque, occupying the remaining part of the optimal control input. Once α increases to 100%, then the takeover process has been completed. The detailed information of each module within this framework is described in the Methods section in the main text.

automation system's control effort according to the measured states and control action of a driver. It also applies an intelligent haptic steering feedback to the driver to ensure that the takeover transition is completed in a safe and smooth manner. A detailed control block diagram of the system is shown in **Figure 2**. Rather than a simple vibration, the proposed intelligent haptic interface is a torque. As shown in **Figure 3**, the functionality of the intelligent haptic torque is divided into two phases: phase 1 haptic guidance and phase 2 haptic assistance. The haptic guidance torque is provided when the driver's control capability is not ideal. It is expected to guide the human driver to properly operate the steering wheel, actively helping to recover the driver's situational awareness and driving ability. When the driver's control capability recovers to a high level, the functionality of the haptic interface switches from guidance to assistance, providing only slight corrections and assisting in smoothing the vehicle trajectory until the takeover is complete. The detailed experimental results and methodology adopted are described later.

2. Results

The feasibility and effectiveness of the proposed intelligent haptic takeover control were investigated by conducting experiments in an automated vehicle (**Figure 4**a,b) involving 26 participants engaged in 2 tasks. The first one was an automation-to-driver takeover control under a single-lane normal steering condition (Task A; Figure 4c), and the second one was an automation-to-driver takeover control under a single-lane change maneuver (Task B; Figure 4d). For comparison, experiments were completed by each participant for each task using two different haptic takeover methods. One proposed method used an intelligent two-phase haptic feedback (Figure 3), and the other was the baseline approach, which consisted of a fade out of the autopilot steering torque (Figure S1, Supporting Information). The order of the experiments for each participant was randomized.

During the experiments, the allowed driver control authority α^{ref}, degree of driver intervention or control performance α, haptic guidance torque T_{hpt}, torque applied to the steering wheel by the driver T_H, and yaw rate $\dot{\psi}$ of the vehicle were recorded for each participant over time (refer to the Methods section for detailed definitions of these variables). Example data of the automation-to-driver takeover process for a representative participant while conducting Task A are shown in **Figure 5**. The experimental results for a representative participant while conducting Task B are shown in Figure S2, Supporting Information. Further statistical analysis of the measured data was conducted for all 26 participants under the designated tasks based on the takeover time, driver steering torque, and yaw rate of the vehicle (Table S1, S2, Supporting Information). The values are presented

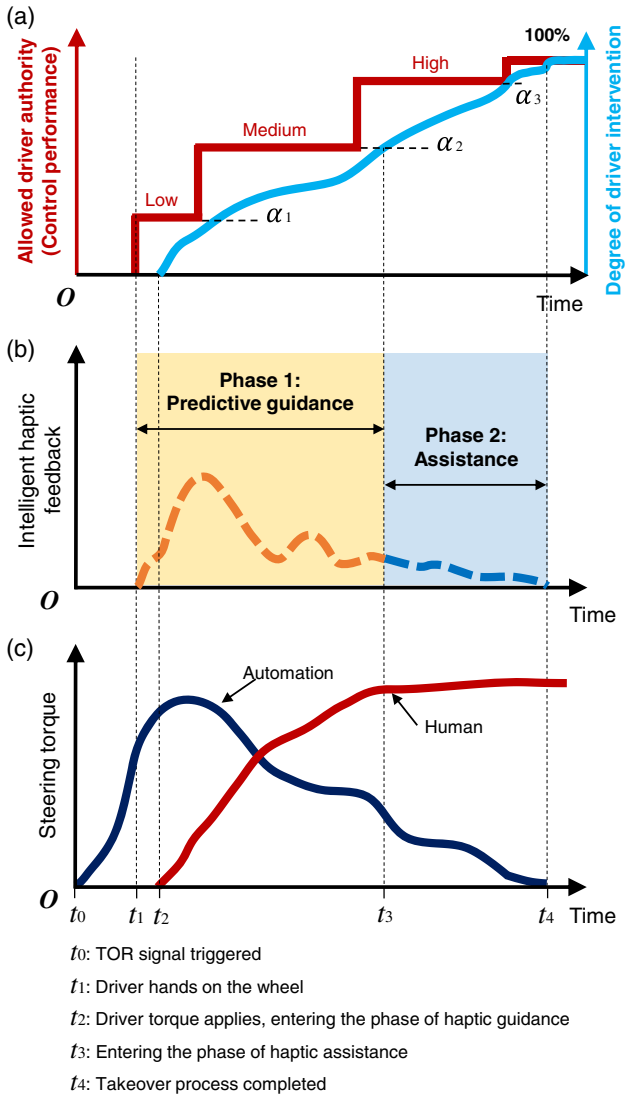

Figure 3. Schematic of the takeover process under the intelligent two-phase haptic interface. a) The allowed control authority gradually increases, with the degree of driver intervention and control performance being increased under the provided haptic feedback. b) Disengaging from the preoccupied NDA and transitioning back to the driving task, when driver's control ability is medium or lower (phase 1), the predictive haptic guidance torque is generated, guiding the driver to properly steer the hand wheel to a suitable position and gradually recovering their situation awareness and their manual control ability. As the states and control performance of the driver recover (phase 2), the functionality of the haptic feedback transitions from guidance to assistance at t_3, only providing slight corrections consistent with the operations of the driver, compensating for the driver's imperfect actions and smoothing vehicle trajectory. c) The driver perceives the TOR signal triggered at t_0, and the hands are detected to be on the steering wheel at t_1. Under the haptic guidance, the driver intervenes in control at t_2. Once the driver's state is considered as fully qualified for manual driving at t_4, the haptic assistance as well as the contribution of automation are removed, and the takeover process is completed.

in the form of the mean ± the standard deviation (SD). The time span used to calculate the mean values of the measured signals was each participant's individual takeover time.

2.1. Takeover Time

The takeover time was recorded and assessed for each participant using the baseline and proposed methods (Table S1, S2, Supporting Information). According to the results shown in **Figure 6**a and **7**a, for the test with the baseline method, the mean value of the takeover time values of all participants was 8.0 ± 0.6 s for Task A and 7.9 ± 0.8 s for Task B. For the test with the proposed method, their mean was 4.4 ± 0.2 s for Task A and 4.4 ± 0.3 s for Task B. The statistical significance of differences in mean values of takeover time under the two approaches was further analyzed using a paired *t*-test. Based on the results, the reduction in takeover time under the proposed method can be regarded as statistically significant ($p < 0.01$).

2.2. Driver Steering Torque

The steering torque T_H applied by the driver was recorded and assessed for each participant during the takeover process under the baseline and proposed methods (Table S1, S2, Supporting Information). As shown in Figure 6b and 7b, for the baseline group, the mean value of the average T_H of all participants was 0.9 ± 0.21 N m for Task A and 0.33 ± 0.1 N m for Task B. Under the proposed method, the mean of the average values of T_H of all participants was 0.8 ± 0.07 N m for Task A and 0.28 ± 0.04 N m for Task B. The statistical significance of the difference in SD values of T_H between the two approaches was analyzed using a paired *t*-test. For both Task A and B, the reductions in the SD values of T_H under the proposed method were considered statistically significant ($p < 0.01$) compared with those obtained in the baseline group.

2.3. Steering Wheel Angle

The steering wheel angle was recorded and assessed for each participant (Table S1 and S2, Supporting Information). As shown in the box plots of Figure 6c and 7c, for the baseline test, the mean of the average values of θ_{sw} across all participants was $13.9° \pm 1.7°$ for Task A and $6.44° \pm 1.6°$ for Task B. Under the proposed method, their mean value was $14.4° \pm 0.7°$ for Task A and $6.39° \pm 0.6°$ for Task B. Significant reductions in SD values of θ_{sw} under the proposed method were identified via a paired *t*-test ($p < 0.01$) compared with the results obtained for the baseline group.

2.4. Yaw Rate of the Vehicle

The yaw rate of the testing vehicle was recorded and assessed for each participant during the takeover process (Table S1 and S2, Supporting Information). As shown in Figure 6d and 7d, under the baseline approach, the mean of the average values of the yaw rate across all participants was $2.3° \pm 0.5° \text{ s}^{-1}$ for Task A and $0.8° \pm 0.37° \text{ s}^{-1}$ for Task B. Under the proposed method, the mean of the average values of the yaw rate across all participants was $2.1° \pm 0.17° \text{ s}^{-1}$ for Task A and $0.7° \pm 0.07° \text{ s}^{-1}$ for Task B. The statistical significance of the reduction in SD values of the yaw rate under the proposed method was also observed via a

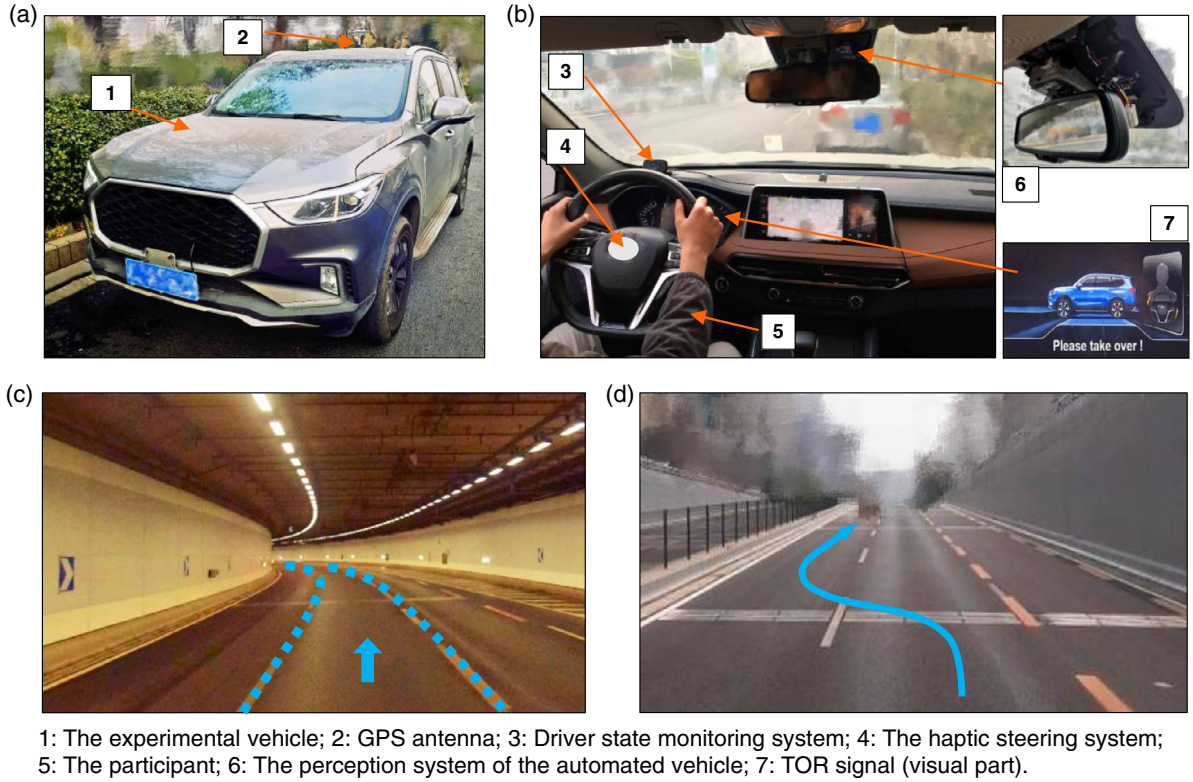

Figure 4. Experimental setup. a) The experimental automated vehicle used in this study was a sport utility vehicle. b) View from inside the testing vehicle. Key components used in the experiment include the driver state monitoring system, haptic steering system, perception system demanded for lane detection of automated vehicle, and TOR signal. c) The scenario of Task A, which was set as the automation-to-driver takeover control during a normal steering maneuver under a single-lane condition. d) The scenario of Task B, which was designed as the automation-to-driver takeover control under a single-lane change maneuver.

paired *t*-test ($p < 0.01$) and compared with the results for the baseline group.

3. Discussion

A comparison of the results shown in Figure 5a indicates that the vehicle trajectory was more consistent under the developed intelligent haptic interface compared with that obtained with the baseline approach, although the representative participant successfully completed Task A while remaining within the lane under both conditions. The results shown in Figure 5b–f demonstrate that the baseline strategy resulted in the driver making many oscillations in the steering torque and angle and that a relatively long time was required to complete the task. As shown in Figure 5g,h, under the proposed strategy, the driver applied the required steering torque smoothly under the guidance and assistance provided by the proposed intelligent haptic interface. This resulted in the driver implementing full manual control within a shorter period of time with little fluctuation in the steering torque and angle, as shown in Figure 5i–k. Similar results were obtained for the same representative participant in Task B (Figure S2, Supporting Information). A statistical analysis of the data like that shown in Figure 5 was conducted for all 26 participants under the designated tasks based on the takeover time, driver steering torque, steering wheel angle, and yaw rate of the vehicle (Table S1, S2, Supporting Information).

Takeover time is an important metric for assessing a driver's takeover ability and takeover performance. A short takeover time could be essential for mitigating the risks associated with particular driving scenarios during the automation-to-driver takeover process in an automated vehicle. In the literature, the takeover time is usually considered as the time span between the TOR and the maneuver commencement as a reaction to the system limit.[10] The threshold values that determine the start of the maneuver were adopted as a 2° steering wheel angle change and 10% brake pedal actuation.[13] However, the start of the maneuver may not be a reasonable condition to indicate the completion of takeover because the driver could lack situational awareness at the initial stage and could therefore not possess the qualifications necessary for safe driving. Instead, we maintain that both starting a control action and the human driver achieving good control performance during the control transition should be considered as the completion of takeover. Thus, in this study, we define the takeover time as the elapsed time between the TOR and the first stabilization of the steering operation (refer to the Statistical Analysis section for a detailed definition). According to the results shown in Figure 6a and 7a, the intelligent two-phase haptic interface generated by the developed human–machine collaboration system reduced the mean

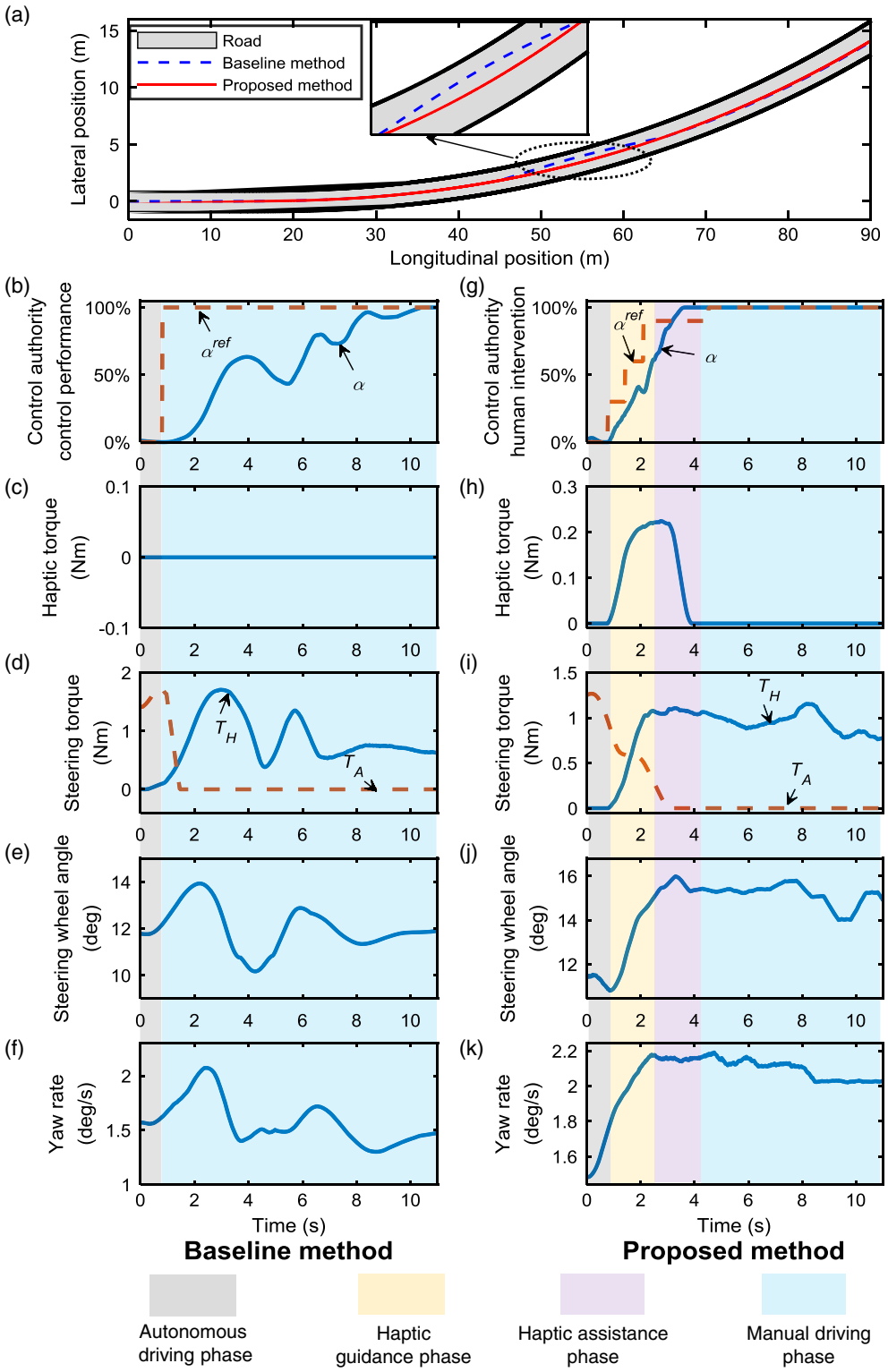

Figure 5. Example data for a representative participant while conducting Task A with baseline and proposed methods. a) The paths of the vehicle during the takeover trails with the participant under the baseline and the proposed methods. b) Allowed driver authority, and the control performance for driving with baseline method. c,h) Haptic torque versus time during each trail. There was no haptic torque applied during takeover with the baseline method. Under the proposed method, the haptic steering torque was generated. d,i) Driver's steering torque and the contribution from automation versus time during each trail. Under the baseline method, the participant made many oscillations in the steering torque to handle the vehicle. With the proposed method, the driver smoothly applied the steering torque under the haptic interface. g) Allowed driver authority, and the degree of driver's intervention versus time during the trail with the proposed method. e,j) The steering angle of the vehicle versus time during each trail. f,k) The yaw rate of the vehicle versus time during each trail.

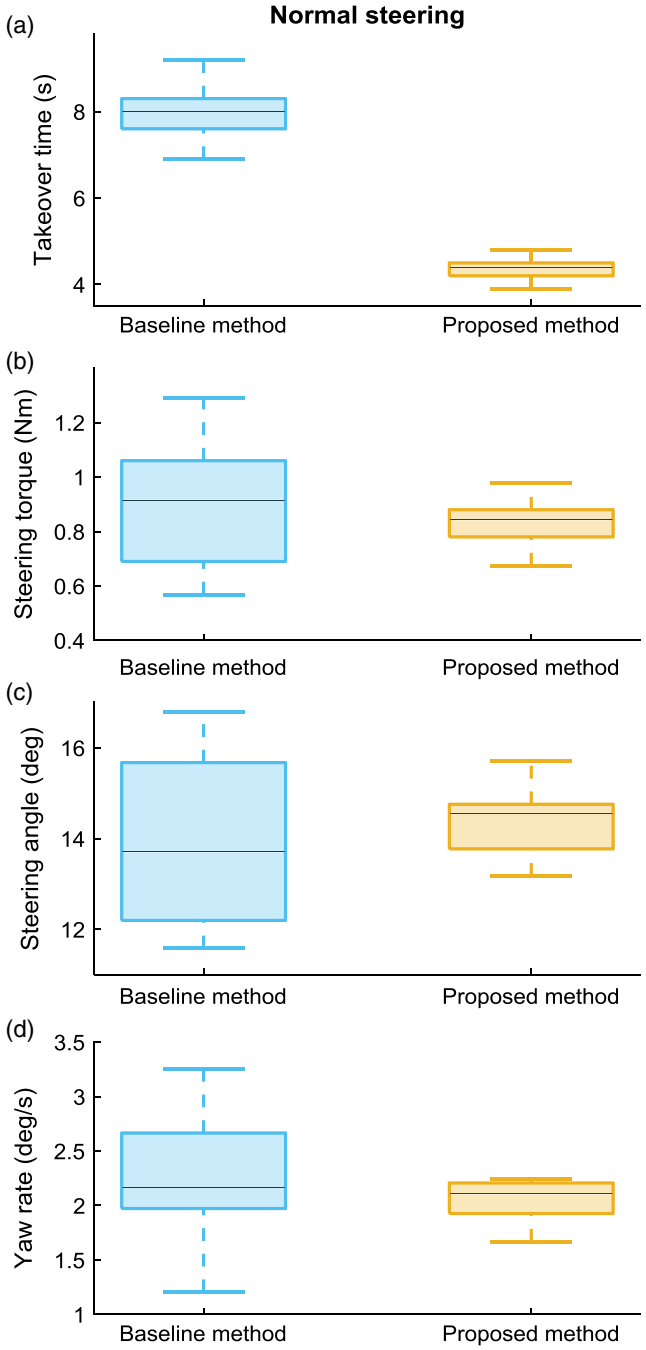

Figure 6. Box plots of the experimental results of Task A. a) Results of takeover time. b) Results of driver steering torque. c) Results of steering wheel angle. d) Results of yaw rate of the vehicle.

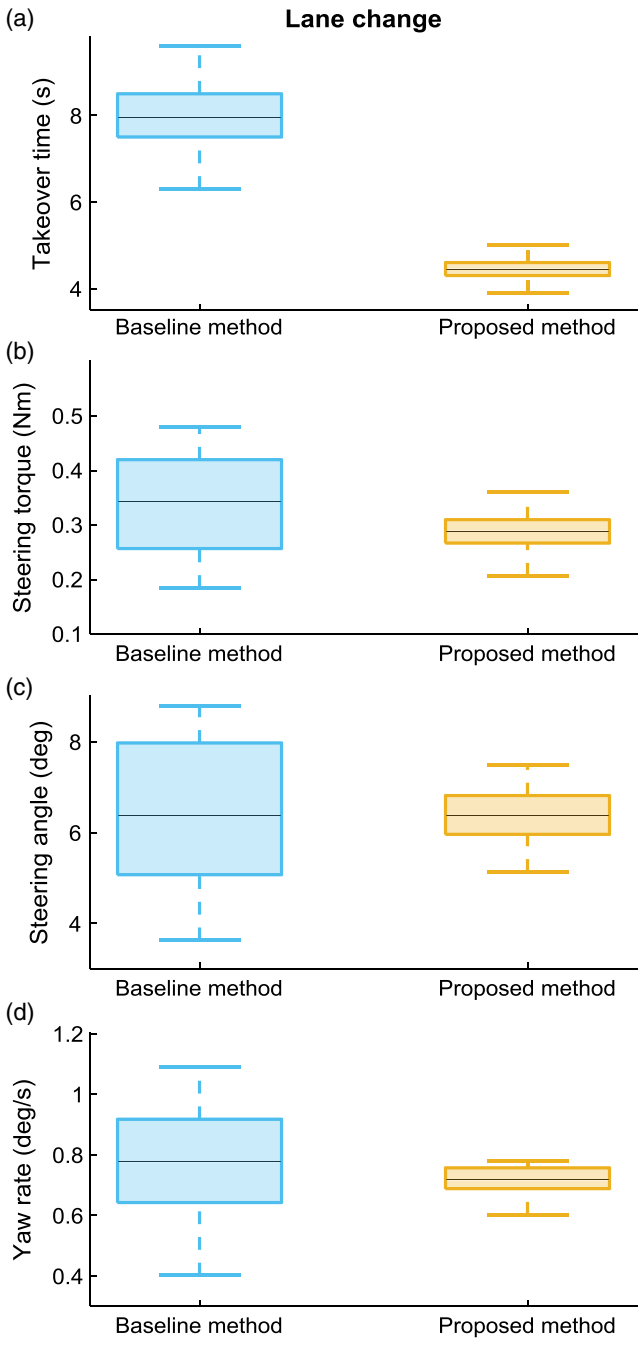

Figure 7. Box plots of the experimental results of Task B. a) Results of takeover time. b) Results of driver steering torque. c) Results of steering wheel angle. d) Results of yaw rate of the vehicle.

takeover time for Task A and B by 51.25% and 44.30%, respectively, compared with the baseline approach.

Takeover control performance is usually related to the difficulty of the required driving task, the cognitive and physical states of the driver, and the skill and experience of the driver. The mean values of the driver steering torque T_H and the steering wheel angle θ_{sw} reflect the required effort of the driving task, whereas the SD is indicative of the consistency of the control performance of each individual driver during the takeover process. It should be noted that the mean values of T_H and θ_{sw} for the baseline and proposed methods in each experimental task were similar according to the results shown in Figure 6b,c and 7b,c. This is because the required action, that is, tracking the lane centerline in Task A, or conducting lane change in Task B, was the same for each test group with the baseline and proposed methods. However, the identified reductions in

SD values of T_H and θ_{sw} under the proposed method suggest that the haptic guidance and assistance provided by the developed system mitigate the impacts of variations in the states and behaviors of the individual drivers on their takeover control performance, ensuring consistency.

The yaw rate $\dot{\psi}$ is indicative of the vehicle maneuverability during the takeover process. The SD values of the yaw rate under the proposed method were significantly lower than those obtained for the baseline group. The relatively high variability of the yaw rate value for each participant in the baseline group also demonstrates the effects of variations in individual driver characteristics and behaviors. The comparison of the results obtained for the two groups demonstrates that the takeover control performances of the drivers were much more consistent under the provided intelligent haptic interface and thus ensure the maneuverability of the vehicle during the takeover process.

In addition, a survey of all participants was conducted after the test runs. The survey results shown in Figure S3, Supporting Information, revealed that the proposed intelligent haptic interface led to a slightly different feeling during takeover transitions but was still regarded as pleasant.

The above experimental results suggest that the proposed intelligent haptic interface can help speed up the driver's driving state recovery and improve the manual control capability during the takeover process. In addition, the high-level control framework, methodology used, and models developed in this work can be expanded to a wide range of human–machine interaction applications.

The design of a human–machine collaboration system for automated vehicles is a systems engineering task that requires the development and cooperation of a number of different areas, such as human factors, control engineering, signal processing, ethics, and law. In the present study, the cognitive and physical states of drivers were considered as discrete levels rather than continuous levels. As such, the coarseness of this discretization may limit the smoothness of the driver state assessment as well as that of the allowed control authority allocation. To further improve the quality of human–machine collaboration, quantitative evaluation of driver states with parameter sensitivity should be investigated in the future. In addition, limiting driver state assessment to only include attention and neuromuscular states may not be a sufficiently complete assessment of the cognitive and physical statuses of the drivers. Therefore, additional signals reflecting the psychological and physiological states of drivers should be included in future studies. We also used a fixed modality, intensity, and frequency for the TOR signal in the experiments. However, this may restrict the possible range of reaction sensitivities available to drivers engaged in different NDAs during the takeover transition. Therefore, adopting a multimodal TOR signal that can adapt to the different NDAs of drivers should be explored. In addition, the experiments conducted in this work only focused on normal driving conditions. In other words, emergency takeovers under critical situations were not considered.

4. Experimental Section

Experimental Design: The experimental sport utility vehicle shown in Figure 4a was modified and used as the testing platform for a range of experiments in automated driving. Technical details with specifications of the testing vehicles are reported in Note S1 and Table S3, Supporting Information.

Two tasks were assigned to the 26 participants (described in detail below), including Task A: automation-to-driver takeover control under a single-lane normal steering condition, and Task B: automation-to-driver takeover control under a single-lane change maneuver. All experiments were conducted in a certified testing area involving three vehicle lanes, each having a uniform width of 3.5 m. Each participant was asked to conduct both Task A and Task B with both takeover control methods. One strategy was the proposed intelligent haptic feedback (Figure 3), whereas the other, namely, the baseline method, used a fade out of the autopilot torque with a fixed slope of 2.5 N m s^{-1} (Figure S1, Supporting Information). For each task, each participant was first asked to naturally drive the testing vehicle for 5 min to get familiar with the car. Then, the participant was required to complete one run for each of the takeover methods. The required tasks as well as the adopted takeover strategies within the experiments for each participant were randomized to avoid learning effects.

The goal of both tasks was for the driver to resume steering control after perceiving a multimodal TOR signal (described in detail later), while ensuring that the designated driving maneuver was accomplished. Before conducting the experiments with the proposed method, the participants were informed that the steering system would provide haptic feedback during the takeover transition. All experiments began with the vehicle stationary on a three-lane roadway. Then, the experimental vehicle was driven in the self-driving mode by the automation system by tracking the centerline of the middle lane of the three-lane roadway, and the vehicle accelerated to the target cruising speed of 10 m s^{-1}. Throughout this period, the human driver was instructed to disregard the roadway and read news on a mobile phone. This designed NDA was cognitively, visually, and physically demanding. The experimenter sat on the rear passenger seat and activated the automatic cruise and lane-keeping functions, thereby enabling autonomous driving in both the longitudinal and lateral directions. For Task A, the roadway for testing had a certain curve with an estimated radius of 190 m. Then, the TOR signal was triggered automatically by the vehicle localization signal at a predefined position. For Task B, the left-turn signal was first engaged at a designated position of a straight section of the roadway. This was a command for the automated driving system to change lanes from the current middle lane to the left one. Then, the TOR signal was automatically triggered after 0.5 s of the left-turn signaling. After perceiving the TOR, the human driver was asked to put the mobile phone down immediately and turn their attention to the driving task in preparation for resuming control of the vehicle. Once the driver was identified to have their hands firmly placed on the steering wheel, the transition of the control authority was triggered. Automatic cruising was performed throughout all the experiments. Thus, each participant was required to only focus on steering control during the takeover action. To ensure consistency in the experiments, the drivers were informed in advance to initiate the takeover action as soon as possible after perceiving the TOR signal. After completion of the maneuver, the driver was asked to engage the brake pedal and bring the vehicle to a complete stop. The subsystems, methods, and algorithms that comprise the above tasks are described in detail below.

In addition, each participant was required to complete a questionnaire after their test runs to gather their personal opinions. The subjects' evaluations were captured via two questions. They were asked whether they noticed a difference between the proposed haptic takeover and the baseline approach, as well as the steering feeling of the proposed one. Both categories were rated on a scale from 1 (no difference/very unpleasant) to 5 (very different/very pleasant).

TOR Signaling: The multimodal TOR signal comprised visual and auditory components that were activated simultaneously. The visual request signal was the text "Please take over!" shown on the dashboard (Figure S4, Supporting Information) until the end of the handover transition. The auditory signal was a 70 dB beep emitted at a frequency of 5 Hz lasting for 0.5 s.

Assessment of Driver States and Control Ability: In the proposed human–machine collaboration system, the control ability of the human driver was

associated with cognitive and physical states assessed online in real time. To simplify the implementation in this study, the focuses of the driver's attention and muscle state in the upper limbs were adopted as indicators of cognitive and physical states, respectively.

For cognitive state assessment, the onboard driver monitoring system (Note S1, Supporting Information) detected the driver's body pose (i.e., driving or NDA), gaze movement, blink frequency, etc., thereby comprehensively assessing the current level (high or low) of the driver's attention to the driving activity. Here, driver attention was deemed low when the driver's current behavior reflected a nondriving or distracted state, such as when the driver was looking down at a mobile phone. In contrast, driver attention was deemed high when the driver's current behavior reflected a normal driving pattern. For example, when reacting to a TOR, the driver would put the mobile phone down and transition to the driving task, checking the mirror and surrounding vehicles.

The muscle state was represented by the neuromuscular dynamics of the driver's arms during steering operations. During the takeover process, a relatively large steering torque may be required to maneuver the vehicle, which would necessitate a relatively large degree of muscle state compared with the more complete muscle relaxation of the nondriving state. To quantitatively assess the degree of muscle state, the neuromuscular dynamics of the driver's arms were characterized and parameterized. To this end, the coupled system of the driver and steering system was abstracted into the following model[30–34]

$$G_s(s) = \frac{\theta_{sw}}{T_H} = \frac{1}{(J_{dr} + J_{st})s^2 + (B_{dr} + B_{st})s + (K_{st} + K_{dr})} \quad (1)$$

where θ_{sw} is the angular position of the steering wheel; T_H is the torque applied to the steering wheel by the driver; J_{dr}, B_{dr}, and K_{dr} are the inertia, viscous damping, and stiffness coefficients of the driver, respectively; and J_{st}, B_{st}, and K_{st} are the inertia, viscous damping, and stiffness coefficients of the steering system, respectively. Existing studies have reported that the value of K is highly correlated with muscle activity during driving, where increasing K reflects increased muscle activity.[32–34] Thus, K was selected as the key indicator of the muscle state. The actual value of K can be estimated online using the existing methods.[33–35] Thus, the level of muscle state (i.e., a driver's physical state) can be considered high when K exceeds a predefined threshold K_1, which was set as 2.5 N m rad^{-1} in the experiments. Otherwise, the driver's physical state is considered to be low, which is indicative of being unqualified for engaging in manual driving.

In the present work, the control ability of a human driver was comprehensively evaluated as low, medium, and high based on the measured levels of the driver's cognitive and physical states according to the scheme shown in **Figure 8**.

Driver Control Authority and Performance: To ensure a safe and smooth transition of control from the autonomous driving mode to the manual driving mode, the maximum allowed control authority α^{ref} ($0 \leq \alpha^{ref} \leq 100\%$) of a human driver is gradually increased before it is entirely given to the driver, setting the upper bound for the degree of the driver's intervention. In the baseline method, the control authority is completely transferred to the driver once the driver intervenes in the control. In the proposed approach, the total driving authority will be gradually allocated to the driver and completely transferred to the driver only after they exhibit the ability to fully qualify for manual driving. Therefore, in this work, based on drivers' different cognitive and physical states, we divided their control ability into three discrete levels, namely, low, medium, and high. Corresponding to these three levels of the driver's control ability, the allowed driver control authority α^{ref} was set to 30%, 60%, and 90% or 100%, respectively. The detailed mechanism for determining α^{ref} based on the driver's state is shown in Figure 8.

In addition, another important state variable α ($0 \leq \alpha \leq 100\%$) indicating the driver's control performance and degree of intervention (or the actual control authority taken by the driver) during takeover is defined here as

$$\alpha = \min\left(\alpha^{ref}, \frac{T_H}{T_{ref}}\right) \quad (2)$$

where T_{ref} is the optimal system input torque, which is sufficient to ensure that the vehicle tracks the lane centerline. In this work, we assumed that the automation system is still working and can calculate T_{ref} within the allowed time budget for takeover. The detailed method and parameters used to compute T_{ref} are reported in Note S2 and in Table S3 and S4, Supporting Information.

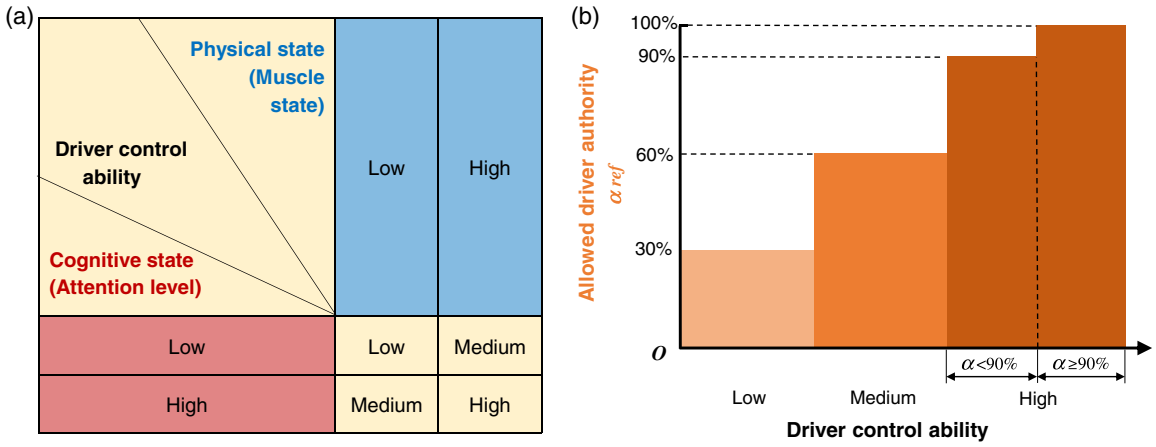

Figure 8. The assessment and decision mechanisms for driver control ability and authority. a) Driver's control ability is assessed based upon the attention level and muscle state. For cognitive state assessment, the onboard driver monitoring system detects the eye gaze direction of the driver as well as the driver's current behavior (i.e., driving or nondriving) and thereby assesses the current level (high or low) of the driver's attention to the driving activity. For physical state assessment, muscle stiffness coefficient K is selected as the key indicator. The level of muscle state is considered high when K exceeds a predefined threshold K_1. Otherwise, the driver's physical state is considered to be low. When both the cognitive and physical states of the driver are low, the driver control ability is considered as low. When only one of the two states is low, the control ability is considered as medium. And when both the cognitive and physical states of the driver are high, then the driver control ability is considered as high. b) The maximum allowed driver control authority α^{ref} is decided based on driver's control ability. When driver's control ability is considered as low, then the value of α^{ref} is set as 30%. When driver's control ability is considered as medium, then the value of α^{ref} is set as 60%. When driver's control ability is considered as high, and the degree of driver's intervention α is below 90%, then the value of α^{ref} is set as 90%. When driver's control ability is considered as high, and the degree of driver's intervention α is 90% and above, then the value of α^{ref} is set as 100%.

In the baseline approach, α can be considered an indicator of the driver's control performance. In the proposed method, α indicates the actual degree of driver intervention. In this work, three threshold parameters of α (shown in Figure 3a) were defined as $\alpha_1 = 30\%$, $\alpha_2 = 60\%$, and $\alpha_3 = 90\%$. After exceeding the predefined threshold α_3, the vehicle can be considered as stabilized and fully controlled by the human driver if and only if α steadily holds within the interval between α_3 and 100% for a period of time (set as 1.5 s in this work). Then, the control authority is entirely transferred to the human driver, and the takeover can be considered completed.

It should be noted that the presented concept of α for assessing the degree of driver intervention will only work if the required steering torque is significantly unequal to zero. However, in a takeover scenario that occurs on a straight road, α cannot be calculated. In this case, indicators that could effectively reflect the driver's takeover performance have to be further explored. Ideally, those would be simple but reliable determination criteria. For example, if the driver puts his hands on the steering wheel, and the steering wheel angle holds within a small interval that is close to the neutral position for a period of time, then the takeover could be considered completed.

Modeling of Human–Machine Collaboration Process: The predictive haptic guidance and assistance controller was designed based on a human–machine interaction model. The model must sufficiently describe the interactive behaviors and shifting roles between humans and automation control under haptic guidance and assistance. In this study, we modeled the driver–automation collaboration as a two-phase process that included automation dominance and human dominance.

1) Automation dominance. The driver's control ability was low in the early stage of takeover, resulting in a low value of α^{ref}. Therefore, automated control should dominate during this stage, and only a small portion of the control authority should be allocated to the human driver.

2) Human dominance. The driver's control ability recovered to a relatively high level in the later stage of takeover, and the value of α^{ref} increased accordingly. Therefore, human driver control should dominate during this stage, with the contribution of automation control decreasing accordingly.

Here, automation dominance is assumed if α is less than the designed threshold α_2, which was set to 60% in the present study. Otherwise, human dominance is assumed.

As presented in the high-level control framework of the system (Figure 2), the input contributed by the automation system T_{A} always compensated for the summation of the driver's actual torque and the haptic torque T_{hpt} during the takeover process, occupying the remaining part of the optimal control input T_{ref}. It was directly applied to the downstream vehicle plant rather than the steering wheel to ensure that the vehicle could track the lane centerline. Thus, the automation torque T_{A} can be expressed as

$$T_{\text{A}} = T_{\text{ref}} - T_{\text{H}} - T_{\text{hpt}} \tag{3}$$

The detailed method of implementing T_{A} and T_{hpt} in the experimental car is reported in Note S1, Supporting Information.

The overall input u to the physical plant of the vehicle is expected to be consistent with the required optimal input T_{ref}, and it can be calculated as

$$u = T_{\text{H}} + T_{\text{A}} + T_{\text{hpt}} \tag{4}$$

where T_{hpt} is the haptic feedback torque. The detailed control algorithm for T_{hpt} is introduced in the following section.

The Two-Phase Predictive Haptic Steering Torque Controller: According to the automation dominance and human dominance phases defined above, the functionality of the haptic takeover controller is classified as: phase 1, predictive haptic guidance; and phase 2, haptic assistance. Disengaging from the preoccupied NDA and transitioning back to the driving task, when the driver's control ability was medium or lower, were still considered to be in the phase of automation dominance. Thus, in phase 1, the haptic feedback torque should be generated based on the estimation of the driver's future reaction using a human model of the automation dominance phase. In this phase, the haptic torque applied to the steering wheel was expected to guide the driver to properly control the steering wheel to a suitable position and simultaneously help recover their situational awareness. As the state and control performance of the driver recover, phase 2 begins, that is, the human dominance phase. Therefore, in phase 2, the functionality of the haptic feedback transitions from guidance to assistance. The assistive torque only provided slight corrections consistent with the operations of the driver, compensating for the driver's imperfect actions, smoothing the vehicle trajectory, and further improving the driver's control performance. Thus, the intelligent two-phase haptic controller was designed as follows:

1) Predictive haptic guidance. An appropriate value of T_{hpt} is generated and applied to the steering system to guide the human driver to steer the vehicle in the proper direction and also impart a better understanding of the required driving task. Assuming that the human driver follows the guidance provided by T_{hpt}, we can describe the dynamics of the interaction between haptic guidance and human action as

$$\lambda \dot{T}_{\text{hpt}} = \tau_{\text{H}} \dot{T}_{\text{H}} + T_{\text{H}} \tag{5}$$

where τ_{H} is a time constant representing the driver's reaction time and λ is a gain representing the amplified influence of T_{hpt} on the driver's activity. To achieve the goal of predictive haptic guidance, an optimization problem is formulated to compute T_{hpt}.[36] Here, the objective function given in Equation 6a is minimized according to the deviation between α^{ref} and α, while being subject to the constraints given by Equations 6b–6e.

$$\min_{T_{\text{hpt},0|k}} \sum_{i=1}^{N} \|\alpha_{i|k} - \alpha_{i|k}^{\text{ref}}\|_{W}^{2} + \sum_{i=0}^{N-1} \|T_{\text{hpt},i|k}\|_{Q}^{2} \tag{6a}$$

$$\text{s.t.} T_{\text{H},i+1|k} = f(T_{\text{H},i|k}, T_{\text{hpt},i|k}) \tag{6b}$$

$$T_{\text{hpt,min}} \leq T_{\text{hpt},i|k} \leq T_{\text{hpt,max}} \tag{6c}$$

$$\Delta T_{\text{hpt,min}} \leq \Delta T_{\text{hpt},i|k} \leq \Delta T_{\text{hpt,max}} \tag{6d}$$

$$\alpha_{0|k} = \alpha_k, \ T_{\text{hpt},-1|k} = T_{\text{hpt},k-1} \tag{6e}$$

where the dynamics model in Equation 6b is obtained by discretizing Equation 5 using the Euler method.[37] The above optimization problem is solved using the model predictive control (MPC) with a moving horizon.[38,39] N is defined as the prediction horizon, W and Q are weighting factors, and $\alpha_{i|k}$ denotes the ith state prediction at time step k obtained by applying the optimal input $\mathbf{u}_k = \{T_{\text{hpt},0|k}, T_{\text{hpt},1|k}, \ldots, T_{\text{hpt},N-1|k}\}$ to Equation 6b beginning from the measured state $T_{\text{hpt},k-1}$ in Equation 6e at the current time step $k-1$. In addition, the constraints on T_{hpt} are explicitly considered in Equation 6c and 6d. The values of the key parameters used in MPC are shown in Table S5, Supporting Information.

2) Haptic assistance. The value of T_{hpt} should be reduced from a guidance role to an assistance role that is consistent with the activities of the human driver, thereby correcting driver activity via compensation. In this functionality, T_{hpt} is designed as

$$T_{\text{hpt}} = \alpha^{\text{ref}} T_{\text{ref}} - T_{\text{H}} \tag{7}$$

If the level of the driver's control ability is considered to be high when the degree of the driver's intervention α exceeds the threshold, $\alpha_3 = 90\%$ (100% will be assigned to α^{ref}, refer to Figure 8 for details), and α steadily holds between 90% and 100% for 1.5 s, then the human driver is considered fully qualified for the required driving task. At this time, the takeover control transition is deemed completed, the haptic steering torque ceases, and the automation system is entirely disengaged.

Participants: A total of 26 participants (16 males, 10 females) in the age range from 22 to 50 (mean = 31.08, SD = 7.23) were recruited for the experiments. Each participant had a valid driving license and signed an informed consent form. The study protocol and consent form were approved by the Nanyang Technological University Institutional Review Board (protocol number IRB-2018-11-025). None of the participants

had previous knowledge of the research topic and had never previously experienced a haptic takeover during driving. Before the experiments, the participants were informed that the steering system would provide haptic feedback during takeover transition.

Statistical Analysis: Statistical analysis of the experimental data was conducted under the designated tasks based on four metrics.

1) Statistical methods. The statistical analysis was performed in Matlab (R2017b, MathWorks) using the Statistics and Machine Learning Toolbox and in Microsoft Excel. Statistical significance was determined using paired *t*-tests at the $\alpha = 0.01$ threshold level throughout the paper. Central tendency was estimated using the mean.

2) Definition of evaluation metrics. Four metrics were adopted to evaluate the takeover performance. The first was the takeover time. In the present work, we define the takeover time as the elapsed time between the TOR and first stabilization of the steering operation. The first stabilization of the steering operation is defined as the point in time when α attained a value between 90% and 100% and was sustained for 1.5 s. Here, the takeover time is a key parameter reflecting the speed at which a human driver achieves a good driving performance from being initially preoccupied with an NDA. The second metric was the driver steering torque, which was applied by the human driver on the steering hand wheel. This directly reflected the driver's actions during the takeover process. The third metric was the steering wheel angle, which was the angular movement of the steering wheel. Because it was a result of both human and automation actions, it can indicate the interactive behavior between the human and machine. The last metric was the yaw rate of the vehicle $\dot{\psi}$, which was the first derivative of the yaw angle of the vehicle (Figure S5, Supporting Information), reflecting the vehicle maneuverability.[40]

Supporting Information

Supporting Information is available from the Wiley Online Library or from the author.

Acknowledgements

This work was supported in part by the SUG-NAP Grant (no. M4082268.050) of Nanyang Technological University, the A*STAR Grant of Singapore (no. 1922500046), the National Nature Science Foundation of China (no. 51875302), and the State Key Laboratory of Automotive Safety and Energy under Project (no. KF2021).

Conflict of Interest

The authors declare no conflict of interest.

Data Availability Statement

The data that support the findings of this study are available from the corresponding author upon reasonable request.

Keywords

automated driving, human–machine collaborations, intelligent haptic interfaces, takeover controls

Received: October 8, 2020
Revised: January 1, 2021
Published online:

[1] A. Nunes, B. Reimer, J. F. Coughlin, *Nature* **2018**, *556*, 169.
[2] K. Goldberg, *Nat. Mach. Intell.* **2019**, *1*, 2.
[3] J. R. Clark, N. A. Stanton, K. M. Revell, *Transp. Res. F: Traffic Psychol. Behav.* **2018**, *65*, 699.
[4] C. Gold, M. Körber, D. Lechner, K. Bengler, *Hum. Factors* **2016**, *58*, 642.
[5] C. Lv, D. Cao, Y. Zhao, D. J. Auger, M. Sullman, H. Wang, L. M. Dutka, L. Skrypchuk, A. Mouzakitis, *IEEE/CAA J. Autom. Sin.* **2018**, *5*, 58.
[6] A. Eriksson, N. A. Stanton, *Hum. Factors* **2017**, *59*, 689.
[7] F. Flemisch, M. Heesen, T. Hesse, J. Kelsch, A. Schieben, J. Beller, *Cognit. Technol. Work* **2012**, *14*, 3.
[8] C. Lv, J. Xue, in *IEEE Intelligent Vehicles Symp. (IV)*, IEEE, Paris **2018**, pp. 1596–1601.
[9] F. O. Flemisch, K. Bengler, H. Bubb, H. Winner, R. Bruder, *Ergonomics* **2014**, *57*, 343.
[10] C. Gold, R. Happee, K. Bengler, *Accid. Anal. Prev.* **2018**, *116*, 3.
[11] M. Kyriakidis, J. C. de Winter, N. Stanton, T. Bellet, B. van Arem, K. Brookhuis, M. H. Martens, K. Bengler, J. Andersson, N. Merat, N. Reed, M. Flament, M. Hagenzieker, R. Happee, *Theor. Issues Ergon. Sci.* **2019**, *20*, 223.
[12] M. Mulder, D. A. Abbink, E. R. Boer, *Hum. Factors* **2012**, *54*, 786.
[13] C. Gold, D. Damböck, L. Lorenz, K. Bengler, in *Proc. of the Human Factors and Ergonomics Society Annual Meeting*, SAGE Publications, Los Angeles, CA **2013**, pp. 1938–1942.
[14] J. Wan, C. Wu, *IEEE Trans. Hum.-Mach. Syst.* **2018**, *48*, 582.
[15] B. Wandtner, N. Schömig, G. Schmidt, *Hum. Factors: J. Hum. Factors Ergon. Soc.* **2018**, *60*, 870.
[16] P. Bazilinskyy, S. M. Petermeijer, V. Petrovych, D. Dodou, J. C. F. de Winter, *Transp. Res. F: Traffic Psychol. Behav.* **2018**, *56*, 82.
[17] J. Radlmayr, C. Gold, L. Lorenz, M. Farid, K. Bengler, in *Proc. of the Human Factors and Ergonomics Society Annual Meeting*, Vol. *58*, Sage Publications, Los Angeles, CA **2014**, pp. 2063–2067.
[18] V. A. Banks, N. A. Stanton, *Theor. Issues Ergon. Sci.* **2019**, *20*, 250.
[19] J. Ludwig, M. Martin, M. Horne, M. Flad, M. Voit, R. Stiefelhagen, S. Hohmann, *Automatisierungstechnik* **2018**, *66*, 146.
[20] J. Nilsson, P. Falcone, J. Vinter, *IEEE Trans. Intell. Transp. Syst.* **2015**, *16*, 1806.
[21] N. Merat, A. H. Jamson, F. C. Lai, O. Carsten, *Hum. Factors* **2012**, *54*, 762.
[22] H. E. Russell, L. K. Harbott, I. Nisky, S. Pan, A. M. Okamura, J. Christian Gerdes, *Sci. Robot.* **2016**, *1*, eaah5682.
[23] T. Saito, T. Wada, K. Sonoda, *IEEE Trans. Intell. Veh.* **2018**, *3*, 198.
[24] M. Mulder, D. A. Abbink, E. R. Boer, in *IEEE Int. Conf. on Systems, Man and Cybernetics*, IEEE, Singapore **2008**, pp. 804–809.
[25] S. M. Erlien, S. Fujita, J. C. Gerdes, *IEEE Trans. Intell. Transp. Syst.* **2016**, *17*, 441.
[26] M. Flad, J. Otten, S. Schwab, S. Hohmann, in *IEEE Int. Conf. on Systems, Man and Cybernetics*, IEEE, San Diego, CA **2014**, pp. 3585–3592.
[27] X. Na, D. Cole, *IEEE Trans. Hum.-Mach. Syst.* **2015**, *45*, 25.
[28] F. Mars, P. Chevrel, *Annu. Rev. Control* **2017**, *44*, 292.
[29] J. Ludwig, C. Gote, M. Flad, S. Hohmann, in *IEEE International Conf. on Systems, Man and Cybernetics*, IEEE, Banff **2017**, pp. 117–122.
[30] J. Ludwig, A. Haas, M. Flad, S. Hohmann, in *IEEE Int. Conf. on Systems, Man, and Cybernetics*, IEEE, Miyazaki **2018**, pp. 3201–3206.
[31] H. J. Ferreau, C. Kirches, A. Potschka, H. G. Bock, M. Diehl, *Math. Program. Comput.* **2014**, *6*, 327.
[32] C. Lv, H. Wang, D. Cao, Y. Zhao, D. J. Auger, M. Sullman, R. Matthias, L. Skrypchuk, A. Mouzakitis, *IEEE/ASME Trans. Mechatron.* **2018**, *23*, 2558.
[33] A. J. Pick, D. J., Cole, *J. Dyn. Syst. Meas. Control* **2008**, *130*, 031004.
[34] A. Pick, Ph.D Dissertation, University of Cambridge **2003**.
[35] A. J. Pick, D. J. Cole, in *The Dynamics of Vehicles on Roads and on Tracks: Proc. of the 18th Int. Symp. of the International Association for Vehicle System Dynamics* **2004**, pp. 182–191.

[36] F. Borrelli, A. Bemporad, M. Morari, *Predictive Control for Linear and Hybrid Systems*, Cambridge University Press, Cambridge **2017**.
[37] S. Gottlieb, C. W. Shu, *Math. Comput.* **1998**, *67*, 73.
[38] D. J. Cole, A. J. Pick, A. M. C. Odhams, *Veh. Syst. Dyn.* **2006**, *44*, 259.
[39] D. J. Cole, *Veh. Syst. Dyn.* **2012**, *50*, 573.
[40] R. Rajamani, *Vehicle Dynamics and Control*, Springer **2011**.

2021-02-12

Human-machine collaboration for automated driving using an intelligent two-phase haptic interface

Lv, Chen

Wiley

Lv C, Li Y, Xing Y, et al., (2021) Human-machine collaboration for automated driving using an intelligent two-phase haptic interface. Advanced Intelligent Systems, Volume 3, April 2021, Article number 2000229

https://doi.org/10.1002/aisy.202000229